LECTURE 12: Loop Antennas

(*Radiation parameters of a small loop. Circular loop of constant current. Equivalent circuit of the loop antenna. The small loop as a receiving antenna. Ferrite loops.*)

1. Introduction

Loop antennas feature simplicity, low cost and versatility. They may have various shapes: circular, triangular, square, elliptical, etc. They are widely used in communication links up to the microwave bands (up to ≈ 3 GHz). They are also used as electromagnetic (EM) field probes in the microwave bands. Electrically small loops are widely used as compact transmitting and receiving antennas in the low MHz range (3 MHz to 30 MHz, or wavelengths of about 10 m to 100 m).

Loop antennas are usually classified as electrically small ($C < \lambda / 3$) and electrically large ($C \sim \lambda$). Here, C denotes the loop's circumference.

The small loops of a single turn have small radiation resistance (< 1 Ω) usually comparable to their loss resistance. Their radiation resistance, however, can be improved by adding more turns. Also, the small loops are narrowband. Typical bandwidths are less than 1%. However, clever impedance matching can provide low-reflection transition from a coaxial cable to a loop antenna with a tuning frequency range as high as 1:10.[1] Moreover, in the HF and VHF bands where the loop diameters are on the order of a half a meter to several meters, the loop can be made of large-diameter tubing or coaxial cable, or wide copper tape, which can drastically reduce the loss.

Fig. 1: Shielded Faraday loops used to inductively feed electrically small loop antennas. [©2012, Frank Dörenberg, used with permission; see https://www.nonstopsystems.com/radio/frank_radio_antenna_magloop.htm. Additional resource: L. Turner VK5KLT, "An overview of the underestimated magnetic loop HF antenna,"]

---

[1] John H. Dunlavy Jr., US Patent 13,588,905: "Wide range tunable transmitting loop antenna", 1967.

The small loops, regardless of their shape, have a far-field pattern very similar to that of a small electric dipole perpendicular to the plane of the loop. This is expected because the small loops are effectively magnetic dipoles. Note, however, that the field polarization is orthogonal to that of the electric dipole (E_φ instead of E_θ).

As the circumference of the loop increases beyond $\lambda/3$, the pattern maximum shifts towards the loop's axis and when $C \approx \lambda$, the maximum of the pattern is along the loop's axis.

2. Radiation Characteristics of a Small Loop

A small loop is by definition a loop of constant current. Its radius must satisfy

$$a < \frac{\lambda}{6\pi} \approx 0.053\lambda, \tag{12.1}$$

or, equivalently, $C < \lambda/3$, in order to be able to approximate its far field as that of an infinitesimal magnetic dipole. The limit (12.1) is mathematically derived later in this Lecture from the first-order approximation of the Bessel function of the first order $J_1(x)$ in the general solution for a loop of constant current.

In fact, to make sure that the current has near-constant distribution along the loop, a tighter limit must be imposed:

$$a < 0.03\lambda, \tag{12.2}$$

or, $C < \lambda/5$. The approximate model of the small loop is the infinitesimal loop (or the infinitesimal magnetic dipole).

The expressions for the field components of an infinitesimal loop of electric current of area A were already derived in Lecture 3. Here, we give only the far-field components of the loop, the axis of which is along z:

$$E_\varphi = \eta\beta^2 \cdot (IA) \cdot \frac{e^{-j\beta r}}{4\pi r} \cdot \sin\theta, \tag{12.3}$$

$$H_\theta = -\beta^2 \cdot (IA) \cdot \frac{e^{-j\beta r}}{4\pi r} \cdot \sin\theta. \tag{12.4}$$

It is obvious that the far-field pattern,

$$\bar{E}_\varphi(\theta) = \sin\theta, \tag{12.5}$$

is identical to that of a *z*-directed infinitesimal electric dipole although the polarization is orthogonal. The power pattern is identical to that of the infinitesimal electric dipole:

$$F(\theta) = \sin^2 \theta. \tag{12.6}$$

<u>Radiated power</u>:

$$\Pi = \oiint \frac{1}{2\eta} | E_\varphi |^2 \cdot \underbrace{r^2 \sin\theta d\theta d\varphi}_{ds},$$

$$\Pi = \frac{1}{12\pi} \eta \beta^4 (IA)^2. \tag{12.7}$$

<u>Radiation resistance</u>:

$$R_r = \eta \frac{8}{3} \pi^3 \left(\frac{A}{\lambda^2} \right)^2. \tag{12.8}$$

In free space, $\eta = 120\pi$ Ω, and

$$R_r \approx 31171 (A / \lambda^2)^2. \tag{12.9}$$

Equation (12.9) gives the radiation resistance of a single loop. If the loop antenna has N turns, then the radiation resistance increases with a factor of N^2 (because the radiated power increases as I^2):

$$R_r = \eta \frac{8}{3} \pi^3 \left(N \frac{A}{\lambda^2} \right)^2. \tag{12.10}$$

The relation in (12.10) implies a handy mechanism to increase R_r and the radiated power Π by using multiple loop windings. Unfortunately, the losses of the loop antenna also increase although only as $\sim N$.

    <u>The directivity</u> is the same as that of an infinitesimal dipole:

$$D_0 = 4\pi \frac{U_{\max}}{\Pi_{rad}} = 1.5. \tag{12.11}$$

3. Circular Loop of Constant Current – General Solution

So far, we have assumed that the loop is of very small radius a, which allows the use of the expressions for the infinitesimal magnetic dipole. Now, we derive

the far field of a circular loop, which might not be necessarily very small, but still has constant current distribution. This derivation illustrates the general loop-antenna analysis as the approach is used in the solutions to circular loop problems of nonuniform distributions, too.

The circular loop can be divided into an infinite number of infinitesimal current elements. With reference to the figure below, the position of a current element in the xy plane is characterized by $0° \leq \varphi' < 360°$ and $\theta' = 90°$. The position of the observation point P is defined by (θ, φ).

The far-field approximations are

$$\left| \begin{array}{l} R \approx r - a\cos\psi, \text{ for the phase term,} \\ \dfrac{1}{R} \approx \dfrac{1}{r}, \text{ for the amplitude term.} \end{array} \right. \tag{12.12}$$
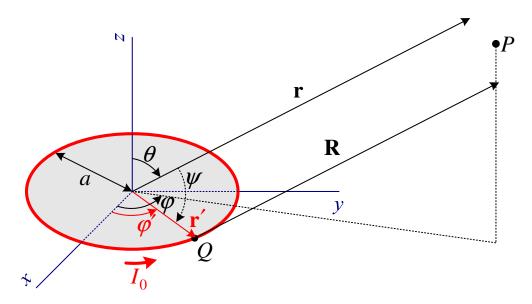
In general, the solution for $\mathbf{A}$ does not depend on φ because of the circular symmetry of the problem. Here, we set $\varphi = 0$. The angle between the position vector of the source point Q and that of the observation point P is determined as

$$\cos\psi = \hat{\mathbf{r}} \cdot \hat{\mathbf{r}}' = (\hat{\mathbf{x}}\sin\theta\underbrace{\cos\varphi}_{1} + \hat{\mathbf{y}}\sin\theta\underbrace{\sin\varphi}_{0} + \hat{\mathbf{z}}\cos\theta) \cdot (\hat{\mathbf{x}}\cos\varphi' + \hat{\mathbf{y}}\sin\varphi'),$$

$$\Rightarrow \cos\psi = \sin\theta\cos\varphi'. \tag{12.13}$$

Now the vector potential integral can be solved for the far zone:

$$\mathbf{A}(r,\theta,0) = \frac{\mu}{4\pi} \oint_C I_0 \frac{e^{-j\beta(r-a\sin\theta\cos\varphi')}}{r} d\mathbf{l}. \tag{12.14}$$

Here, $d\mathbf{l} = \hat{\boldsymbol{\varphi}}' a\, d\varphi'$ is the linear element of the loop contour. The current element changes its direction along the loop and its contribution depends on the angle between its direction and the computed $\mathbf{A}$ vector. Due to the circular symmetry, we conclude that $\mathbf{A}$ has only a φ-component, i.e., $\mathbf{A} = A_\varphi \hat{\boldsymbol{\varphi}}$. From (12.14),

$$A_\varphi(r,\theta,0) = \hat{\boldsymbol{\varphi}} \cdot \mathbf{A}(r,\theta,0) = \frac{\mu}{4\pi}(I_0 a)\frac{e^{-j\beta r}}{r}\int_0^{2\pi}(\hat{\boldsymbol{\varphi}}\cdot\hat{\boldsymbol{\varphi}}')e^{j\beta a\sin\theta\cos\varphi'}d\varphi'. \quad (12.15)$$

Since

$$\begin{aligned}\hat{\boldsymbol{\varphi}}\cdot\hat{\boldsymbol{\varphi}}' &= (\hat{\mathbf{x}}\cos\varphi + \hat{\mathbf{y}}\sin\varphi)\cdot(\hat{\mathbf{x}}\cos\varphi' + \hat{\mathbf{y}}\sin\varphi') = \\ &= \cos\varphi\cos\varphi' + \sin\varphi\sin\varphi' = \\ &= \cos(\varphi-\varphi')\big|_{\varphi=0} = \cos\varphi',\end{aligned} \quad (12.16)$$

the vector potential is

$$A_\varphi(r,\theta,0) = \frac{\mu}{4\pi}(I_0 a)\frac{e^{-j\beta r}}{r}\int_0^{2\pi}\cos\varphi'\cdot e^{j\beta a\sin\theta\cos\varphi'}d\varphi', \quad (12.17)$$

$$A_\varphi(r,\theta,0) = \frac{\mu}{4\pi}(I_0 a)\frac{e^{-j\beta r}}{r}\left[\int_0^{\pi}\cos\varphi'\cdot e^{j\beta a\sin\theta\cos\varphi'}d\varphi' + \int_\pi^{2\pi}\cos\varphi'\cdot e^{j\beta a\sin\theta\cos\varphi'}d\varphi'\right].$$

We apply the following substitution in the second integral: $\varphi' = \varphi'' + \pi$. Then,

$$A_\varphi(\theta) = \frac{\mu I_0 a}{4\pi}\frac{e^{-j\beta r}}{r}\left[\int_0^{\pi}\cos\varphi'\cdot e^{j\beta a\sin\theta\cos\varphi'}d\varphi' - \int_0^{\pi}\cos\varphi''\cdot e^{-j\beta a\sin\theta\cos\varphi''}d\varphi''\right]. \quad (12.18)$$

The integrals in (12.18) can be expressed in terms of Bessel functions, which are defined as

$$\int_0^{\pi}\cos(n\varphi)e^{jz\cos\varphi}d\varphi = \pi j^n J_n(z). \quad (12.19)$$

Here, $J_n(z)$ is the Bessel function of the first kind of order n. From (12.18) and (12.19), it follows that

$$A_\varphi(r,\theta,0) = \frac{\mu}{4\pi}(I_0 a)\frac{e^{-j\beta r}}{r}\pi j\left[J_1(\beta a\sin\theta) - J_1(-\beta a\sin\theta)\right]. \quad (12.20)$$
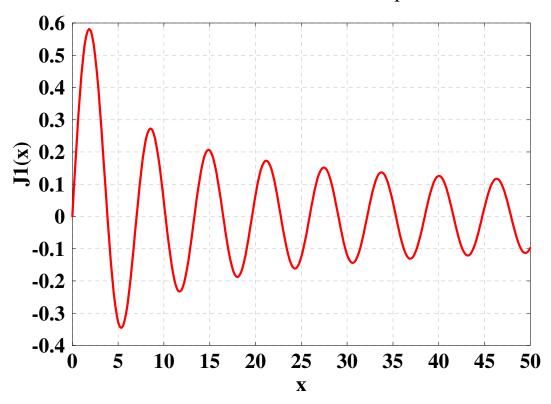
Since

$$J_n(-z) = (-1)^n J_n(z), \tag{12.21}$$

equation (12.20) reduces to

$$A_\varphi(\theta) = j\frac{\mu}{2}(I_0 a)\frac{e^{-j\beta r}}{r}J_1(\beta a \sin\theta). \tag{12.22}$$

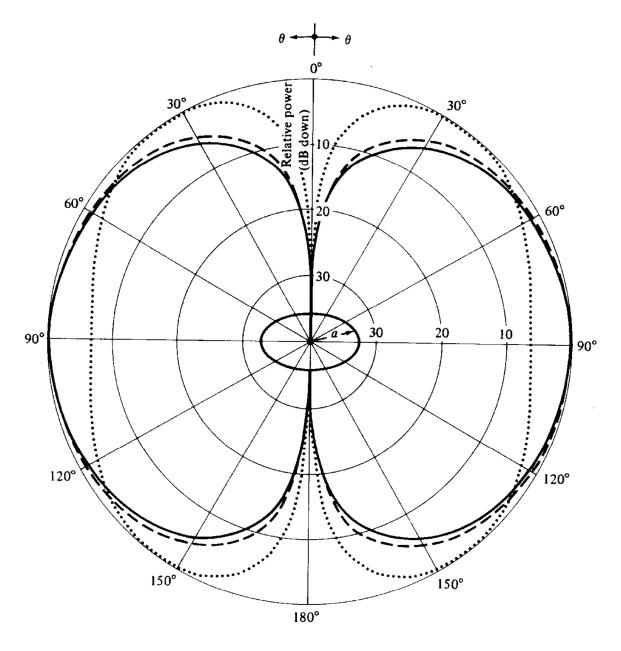The Bessel function of the first kind of order $n = 1$ is plotted below.

Now, the far-zone field components are derived as

$$\left|\begin{array}{l} E_\varphi(\theta) = \beta\eta(I_0 a)\dfrac{e^{-j\beta r}}{2r}J_1(\beta a \sin\theta), \\[3mm] H_\theta(\theta) = -\dfrac{E_\varphi}{\eta} = -\beta(I_0 a)\dfrac{e^{-j\beta r}}{2r}J_1(\beta a \sin\theta). \end{array}\right. \tag{12.23}$$

The patterns of constant-current loops obtained from (12.23) are shown below:

- ————— $a = 0.1\lambda$
- – – – – – $a = 0.2\lambda$
- ·············· $a = 0.5\lambda$

[Balanis]

The small-loop field solution in (12.3)-(12.4) is actually a first-order approximation of the solution in (12.23). This becomes obvious when the Bessel function is expanded in series as

$$J_1(\beta a \sin\theta) = \frac{1}{2}(\beta a \sin\theta) - \frac{1}{16}(\beta a \sin\theta)^3 + \cdots. \qquad (12.24)$$

For small values of the argument ($\beta a < 1/3$), the first-order approximation is acceptable, i.e.,

$$J_1(\beta a \sin\theta) \approx \frac{1}{2}(\beta a \sin\theta). \tag{12.25}$$

The substitution of (12.25) in (12.23) yields (12.3)-(12.4).

It can be shown that the maximum of the pattern given by (12.23) is in the direction $\theta = 90°$ for all loops, which have circumference $C < 1.84\lambda$.

Radiated power and radiation resistance

We substitute the E_φ expression (12.23) in

$$\Pi = \oiint \frac{1}{2\eta} |E_\varphi|^2 \cdot \underbrace{r^2 \sin\theta d\theta d\varphi}_{ds},$$

which yields

$$\Pi = \frac{(\omega\mu)^2}{4\eta}(I_0^2 A) \cdot \int_0^\pi J_1^2(\beta a \sin\theta) \sin\theta d\theta. \tag{12.26}$$

Here, $A = \pi a^2$ is the loop's area. The integral in (12.26) does not have a closed form solution although it can be reduced to a highly convergent series:

$$\int_0^\pi J_1^2(\beta a \sin\theta) \sin\theta d\theta = \frac{1}{\beta a} \int_0^{2\beta a} J_2(x) dx = \frac{2}{\beta a} \sum_{m=0}^\infty J_{2m+3}(2\beta a). \tag{12.27}$$

The radiation resistance is obtained as

$$R_r = \frac{2\Pi}{I_0^2} = \frac{(\omega\mu)^2}{2\eta} A \cdot \int_0^\pi J_1^2(\beta a \sin\theta) \sin\theta d\theta. \tag{12.28}$$

The radiation resistance of small loops is very small. For example, for $\lambda/100 < a < \lambda/30$ the radiation resistance varies from $\approx 3\times10^{-3}$ Ω to ≈ 0.5 Ω. This is often less than the loss resistance of the loop. That is why small loop antennas are constructed with multiple turns and on ferromagnetic cores. Such loop antennas have large inductive reactance, which is compensated by a capacitor. This is convenient in narrowband receivers, where the antenna itself is a very efficient filter (together with the tuning capacitor), which can be tuned for

different frequency bands. Low-loss capacitors must be used to prevent further increase in the loss.

4. Circular Loop of Nonuniform Current

When the loop radius becomes larger than 0.2λ, the non-uniformity of the current distribution cannot be ignored. A common assumption is the cosine distribution.[2,3] Lindsay, Jr.,[4] considers the circular loop to be a deformation of a shorted parallel-wire line. If I_s is the current magnitude at the "shorted" end, i.e., the point opposite to the feed point where $\varphi' = \pi$, then

$$I(\alpha) = I_s \cosh(\gamma a \alpha) \tag{12.29}$$

where $\alpha = \pi - \varphi'$ is the angle with respect to the shorted end, γ is the line propagation constant and a is the loop radius. If we assume loss-free transmission-line model, then $\gamma = j\beta$ and $\cosh(\gamma a \alpha) = \cos(\beta a \alpha)$. For a loop in open space, β is assumed to be the free-space wave number ($\beta = \omega\sqrt{\mu_0 \varepsilon_0}$).

The cosine distribution is not very accurate, especially close to the terminals, and this has a negative impact on the accuracy of the computed input impedance. This situation is similar to the assumption of a sinusoidal current distribution on an electrical dipole, which, too, is not accurate at the dipole's terminals. For this reason, in loops, the current is often represented by a Fourier series:[5,6]

$$I(\varphi') = I_0 + 2\sum_{n=1}^{N} I_n \cos(n\varphi'). \tag{12.30}$$

Here, φ' is measured from the feed point. This way, the derivative of the current distribution with respect to φ' at $\varphi' = \pi$ (the point diametrically opposite to the feed point) is always zero. This imposes the requirement for a symmetrical current distribution on both sides of the diameter from $\varphi' = 0$ to $\varphi' = \pi$. The complete analysis of this general case will be left out, and only some important results will be given. When the circumference of the loop approaches λ, the maximum of the radiation pattern shifts exactly along the loop's normal. Then,

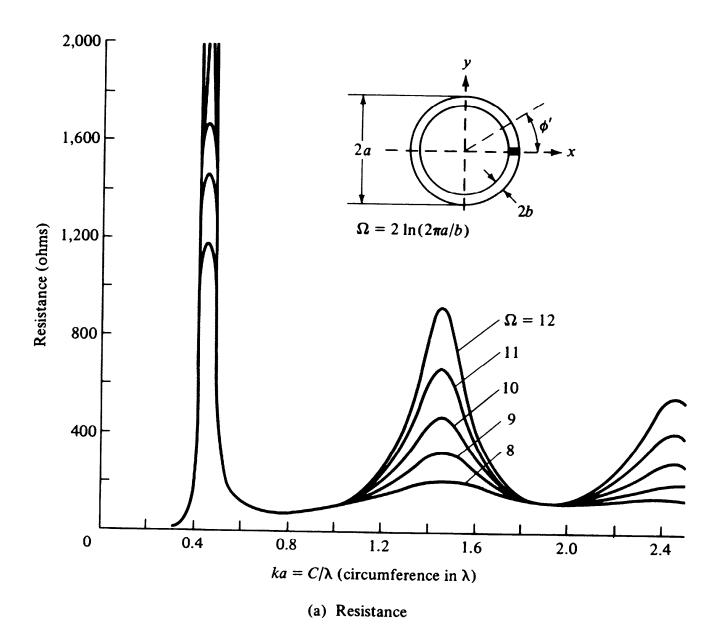[2] E.A. Wolff, *Antenna Analysis*, Wiley, New York, 1966.
[3] A. Richtscheid, "Calculation of the radiation resistance of loop antennas with sinusoidal current distribution," *IEEE Trans. Antennas Propagat.*, Nov. 1976, pp. 889-891.
[4] J. E. Lindsay, Jr., "A circular loop antenna with non-uniform current distribution," *IRE Trans. Antennas Propagat.*, vol. AP-8, No. 4, July 1960, pp. 439-441.
[5] H. C. Pocklington, "Electrical oscillations in wire," in *Cambridge Phil. Soc. Proc.*, vol. 9, 1897, pp. 324–332.
[6] J. E. Storer, "Input impedance of circular loop antennas," *Am. Inst. Electr. Eng. Trans.*, vol. 75, Nov. 1956.

the input resistance of the antenna is also good (about 50 to 70 Ω). The maximum directivity occurs when $C \approx 1.4\lambda$ but then the input impedance is too large. The input resistance and reactance of the large circular loop are given below.
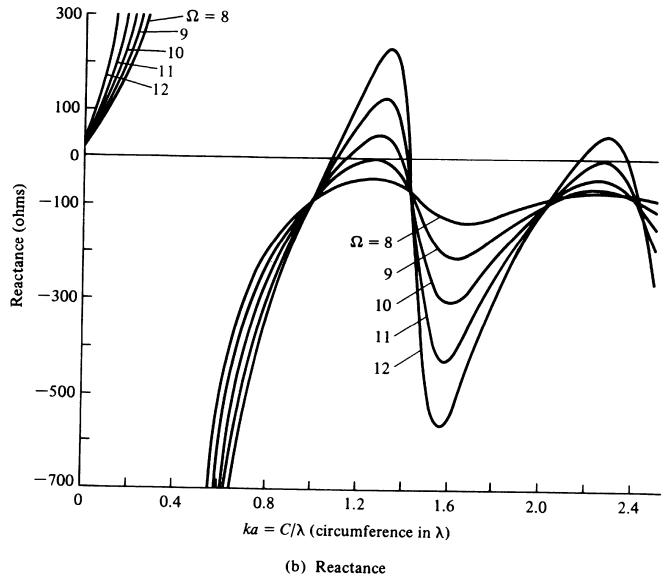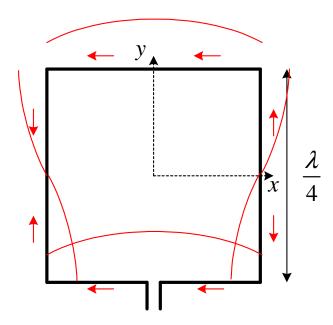

(a) Resistance

(b) Reactance

Figure 5.11 Input impedance of circular loop antennas. (SOURCE: J. E. Stover, "Impedance of Thin-Wire Loop Antennas," *AIEE Trans.,* Vol. 75, November 1956. © 1956 IEEE).

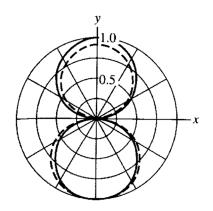(Note: typo in author's name, read as J. E. Storer)

The large circular loop is very similar in its performance to the large square loop. An approximate solution of very good accuracy for the square-loop antenna can be found in

W.L. Stutzman and G.A. Thiele, *Antenna Theory and Design*, 2nd Ed., John Wiley & Sons, New York, 1998.
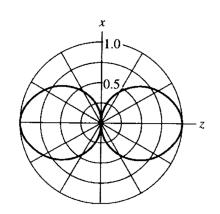
There, it is assumed that the total antenna loop is exactly one wavelength and has a cosine current distribution along the loop's wire.
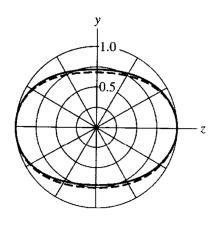

The principal plane patterns obtained through the cosine-current assumption (solid line) and using numerical methods (dash line) are shown below:
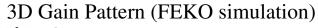

(a) The xy-plane (the plane of the loop and an E-plane) normalized pattern plot of E_ϕ. In this plane, HP = 94°.
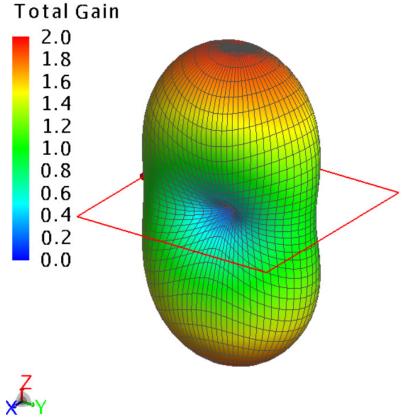
(b) The xz-plane (an E-plane) normalized pattern plot of E_θ. In this plane, HP = 85°. The patterns from the two methods coincide in this plane.
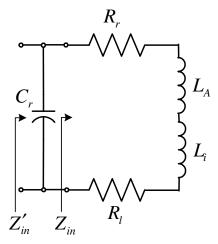
(c) The yz-plane (the H-plane) pattern plot of E_ϕ.

3D Gain Pattern (FEKO simulation)

5. Equivalent Circuit of a Loop Antenna

C_r - resonance (tuning) capacitor

R_l - loss resistance of the loop antenna

R_r - radiation resistance
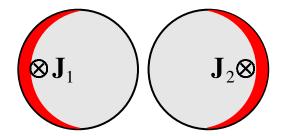
L_A - inductance of the loop

L_i - inductance of the loop conductor (wire)

(a) Loss resistance

Usually, it is assumed that the loss resistance of a loosely wound loop equals the high-frequency loss resistance of a straight wire of the same length as the loop and of the same current distribution. In the case of a uniform current distribution on the contour of the wire's cross-section, the high-frequency resistance is calculated as

$$R_{hf} = \frac{l}{p} R_s, \quad R_s = \sqrt{\frac{\pi f \mu}{\sigma}}, \quad \Omega \qquad (12.31)$$

where l is the length of the wire, and p is the perimeter of the wire's cross-section. We are not concerned with the current distribution along the wire's length now because it can be always taken into account in the same way as it is done for the dipole/monopole antennas. However, another important phenomenon must be taken into account, namely the **proximity effect**, which distorts the uniformity of the current density distribution along the contour of the wire's cross-section as shown below.

When the spacing between the turns of the wound wire is very small, the EM field is strongly suppressed in-between the wires, reducing its ability to drive the high-frequency current on the adjacent metal surfaces. Thus, the loss resistance is made much worse by the proximity effect compared to the skin effect alone. The following formula is used to calculate the loss resistance of a loop with N turns, wire radius b, and turn separation $2c$:

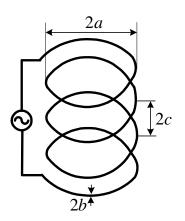$$R_l = \underbrace{\frac{Na}{b} R_s}_{R_{hf}} \left(\frac{R_p}{R_0} + 1 \right) \qquad (12.32)$$

where

$R_s, \quad \Omega$, is the surface resistance (see (12.31)),

R_p, Ω / m, is the equivalent loss resistance per unit length due to the proximity effect,

$R_0 = NR_s / (2\pi b) = R_{hf} / l$, Ω / m, is the loss resistance per unit length due to the skin effect; see R_{hf} in (12.31).

Note that the ratio $Na / b = N \cdot 2\pi a / (2\pi b) = l / p$ is the ratio of the total wire length l to the perimeter p of its cross-section and, therefore, the term in front of the brackets in (12.32) is the high-frequency loss resistance R_{hf} in (12.31).
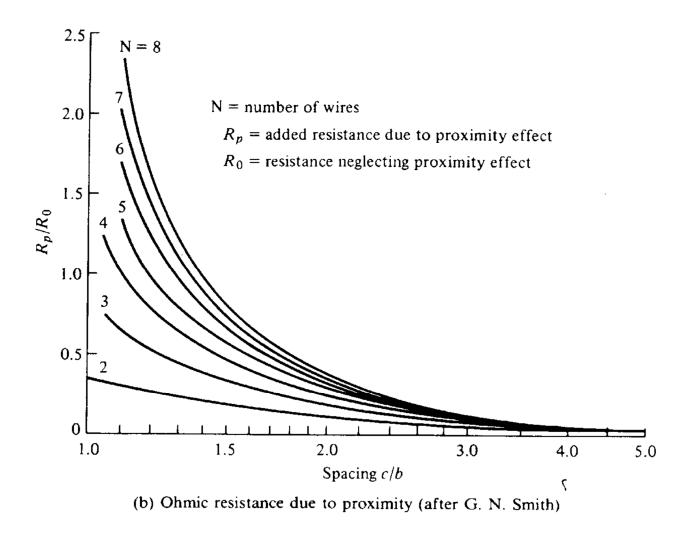

Thus, (12.32) can also be written as

$$R_l = R_{hf}\left(\frac{R_p \cdot l}{R_{hf}} + 1\right) \quad (12.33)$$

which clarifies the meaning of the term in the brackets as a correction factor for the loss resistance R_{hf}, which takes into account only the skin effect.

The ratio R_p / R_0 has been calculated for different relative spacings c / b, for loops with $2 \le N \le 8$ in:

G.N. Smith, "The proximity effect in systems of parallel conductors," *J. Appl. Phys.*, vol. 43, No. 5, May 1972, pp. 2196-2203.

The results are shown in the figure below.

N = 8

7

N = number of wires

R_p = added resistance due to proximity effect

R_0 = resistance neglecting proximity effect

(b) Ohmic resistance due to proximity (after G. N. Smith)

(b) Loop inductance

The inductance of a single circular loop of radius a made of wire of radius b is

$$L_{A1}^{\text{circ}} = \mu a \left[\ln\left(\frac{8a}{b}\right) - 2 \right], \text{ H.} \tag{12.34}$$

The inductance of a square loop with sides a and wire radius b is calculated as

$$L_{A1}^{\text{sq}} = 2\mu \frac{a}{\pi} \left[\ln\left(\frac{a}{b}\right) - 0.774 \right], \text{ H.} \tag{12.35}$$

The inductance of a multi-turn coil is obtained from the inductance of a single-turn loop multiplied by N^2, where N is the number of turns.

The inductance of the wire itself (internal inductance) is very small and is often neglected. It can be shown that the HF self-inductance per unit length of a straight wire of cylindrical cross-section is

$$L'_{int} = \frac{\mu_0}{8\pi}\left[\frac{b^4 - 4b^2c^2 + 3c^4 + 4c^4\ln(b/c)}{(b^2 - c^2)^2}\right], \text{ H/m}, \tag{12.36}$$

where $c = b - \delta$ and δ is the skin depth. To obtain the total internal inductance of the wire, simply multiply L'_{int} by the overall length of the wire used to construct the multi-turn loop antenna.

(c)   Tuning capacitor

The susceptance of the capacitor B_r must be chosen to eliminate the susceptance of the loop. Assume that the equivalent admittance of the loop is

$$Y_{in} = \frac{1}{Z_{in}} = \frac{1}{R_{in} + jX_{in}} \tag{12.37}$$

where

$$R_{in} = R_r + R_l,$$

$$X_{in} = j\omega(L_A + L_{int}).$$

The following transformation holds:

$$Y_{in} = G_{in} + jB_{in} \tag{12.38}$$

where

$$G_{in} = \frac{R_{in}}{R_{in}^2 + X_{in}^2}, \quad B_{in} = \frac{-X_{in}}{R_{in}^2 + X_{in}^2}. \tag{12.39}$$

The susceptance of the capacitor is

$$B_r = \omega C_r. \tag{12.40}$$

For resonance to occur at $f_0 = \omega_0/(2\pi)$ when the capacitor is in parallel with the loop, the condition

$$B_r = -B_{in} \tag{12.41}$$

must be fulfilled. Therefore,

$$2\pi f_0 C_r = \frac{X_{in}}{R_{in}^2 + X_{in}^2}, \tag{12.42}$$

$$\Rightarrow C_r = \frac{1}{2\pi f} \frac{X_{in}}{\left(R_{in}^2 + X_{in}^2\right)}. \tag{12.43}$$

Under resonance, the input impedance Z_{in}' becomes

$$Z_{in}' = R_{in}' = \frac{1}{G_{in}'} = \frac{1}{G_{in}} = \frac{R_{in}^2 + X_{in}^2}{R_{in}}, \tag{12.44}$$

$$\Rightarrow Z_{in}' = R_{in} + \frac{X_{in}^2}{R_{in}}, \quad \Omega. \tag{12.45}$$

5. The Small Loop as a Receiving Antenna
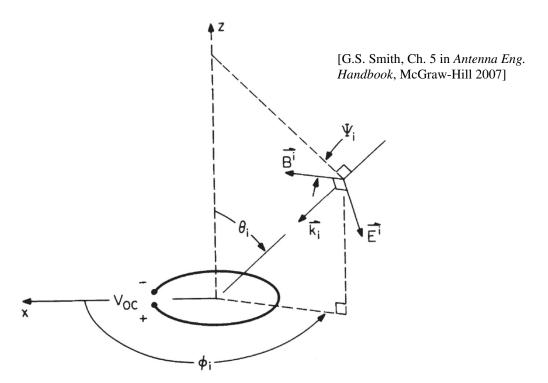
The small loop antennas have the following features:

1) good radiation resistance provided multi-turn ferrite-core constructions are used;

2) high losses, therefore, low radiation efficiency;

3) simple construction, small size and weight.

Small loops are usually not used as transmitting antennas due to their low efficiency. However, they are much preferred as receiving antennas in AM radio-receivers because of their high signal-to-noise ratio (they can be easily tuned to form a very high-Q resonant circuit), their small size and low cost.

Loops are constructed as magnetic field probes to measure magnetic flux densities. At higher frequencies (UHF and microwave), loops are used to measure the EM field intensity. In this case, ferrite rods are not used.

Since the loop is a typical linearly polarized antenna, it has to be oriented properly to optimize reception. The optimal case is a linearly polarized wave with the **H**-field aligned with the loop's axis.

The open-circuit voltage at the loop terminals is induced by the time-varying magnetic flux through the loop:

$$V_{oc} = j\omega \Psi_m = j\omega \mathbf{B} \cdot \mathbf{s} = j\omega \mu H_z \cdot \pi a^2, \qquad (12.46)$$

$$H_z = H^i \cos\psi \sin\theta_i. \qquad (12.47)$$

Here,

Ψ_m is the magnetic flux, Wb;

θ_i is the angle between z (the loop's axis) and the Poynting vector of the incident wave;

φ_i is the angle between the x axis (defined by the center of the loop and the feed point) and the plane of incidence (the plane defined by the z axis and the Poynting vector $\mathbf{P}_i$ (or the wave vector $\mathbf{k}_i$));

ψ is the angle between the $\mathbf{H}^i$ vector and the plane of incidence.

Finally, the open-circuit voltage can be expressed as

$$V_{oc} = j\omega \mu S H^i \cos\psi \sin\theta_i = j\beta S E^i \cos\psi \sin\theta_i. \qquad (12.48)$$

Here, $S = \pi a^2$ denotes the area of the loop, and $\beta = \omega\sqrt{\mu\varepsilon}$ is the phase constant. V_{oc} is maximum for $\theta_i = 90°$ and $\psi = 0°$.

6. Ferrite Loops

The radiation resistance and radiation efficiency can be raised by inserting a ferrite core, which has high magnetic permeability in the operating frequency band. Large magnetic permeability $\mu = \mu_0 \mu_r$ means large magnetic flux Ψ_m, and therefore large induced voltage V_{oc}. The radiation resistance of a small loop was already derived in (12.10) to include the number of turns, and it was shown that it increases as $\sim N^2$. Now the magnetic properties of the loop will be included in the expression for R_r.

The magnetic properties of a ferrite core depend not only on the relative magnetic permeability μ_r of the material it is made of but also on its geometry. The increase in the magnetic flux is then more realistically represented by the ***effective*** *relative permeability* $\mu_{r_{eff}}$. We show next that the radiation resistance of a ferrite-core loop is $(\mu_{r_{eff}})^2$ times larger than the radiation resistance of the air-core loop of the same geometry. When we calculated the far fields of a small loop, we used the equivalence between an electric current loop and a magnetic current element:

$$j\omega\mu(IA) = I_m l . \qquad (12.49)$$

From (12.49) it is obvious that the equivalent magnetic current is proportional to μ. The field magnitudes are proportional to I_m, and therefore they are proportional to μ as well. This means that the radiated power Π_{rad} is proportional to μ^2, and therefore the radiation resistance increases as $\sim (\mu_{r_{eff}})^2$.

Finally, we can express the radiation resistance as

$$R_r = \eta_0 \frac{8}{3}\pi^3 \left(N\mu_{r_{eff}} \frac{A}{\lambda^2} \right)^2 . \qquad (12.50)$$

Here, A is the loop cross-sectional area, and $\eta_0 = \sqrt{\mu_0 / \varepsilon_0}$ is the intrinsic impedance of vacuum. An equivalent form of (12.50) is

$$R_r \approx 20\pi^2 (N\mu_{r_{eff}})^2 \left(\frac{C}{\lambda} \right)^4 \qquad (12.51)$$

where we have used the approximate expression $\eta_0 \approx 120\pi$ and C is the circumference of the loop, $C = 2\pi a$.

Some notes are made below with regard to the properties of ferrite cores:

- The effective magnetic constant of a ferrite core is always less than the magnetic constant of the ferromagnetic material it is made of, i.e., $\mu_{r_{eff}} < \mu_r$. Toroidal cores have the highest $\mu_{r_{eff}}$, and ferrite-stick cores have the lowest $\mu_{r_{eff}}$.

- The effective magnetic constant is frequency dependent. One has to be careful when picking the right core for the application at hand.

- The magnetic losses of ferromagnetic materials increase with frequency. At very high (microwave) frequencies, the magnetic losses are very high. They have to be calculated and represented in the equivalent circuit of the antenna as a shunt conductance G_m.